European Polymer Journal 115 (2019) 138–146

Contents lists available at ScienceDirect

European Polymer Journal

journal homepage: www.elsevier.com/locate/europolj

Exploring the potential of gas-phase esterification to hydrophobize the surface of micrometric cellulose particles

Grégoire David[a], Nathalie Gontard[a], David Guerin[b], Laurent Heux[c], Jérôme Lecomte[a,d], Sonia Molina-Boisseau[c], Hélène Angellier-Coussy[a,*]

[a] JRU IATE 1208 – Univ Montpellier, CIRAD, INRA, Montpellier SupAgro, 2 Place Pierre Viala, Bat 31, F-34060 Montpellier 01, France
[b] CTP, Centre Technique du Papier, CS90251, Domaine Universitaire, Grenoble, France
[c] CNRS, CERMAV, Univ. Grenoble Alpes, 38000 Grenoble, France
[d] CIRAD, UMR IATE, F-34398 Montpellier, France

ARTICLE INFO

Keywords:
Cellulose
Gas-phase esterification
Degree of substitution
Surface free energy
Crystallinity
Water vapor sorption

ABSTRACT

In order to lift the barrier of a poor interfacial interaction between cellulosic plant fibers and polymeric matrices in biocomposites, an eco-friendly surface modification of fibers was explored. A solvent-free gas-phase esterification applied to cellulose particles allowed to graft palmitoyl moieties on their surface in order to make them more compatible with non-polar polymers for composite applications. The efficiency of the treatment was evidenced from FT-IR analysis, and the degree of substitution (DS) was quantified by solid-state ^{13}C NMR spectroscopy. The effect of surface grafting on resulting intrinsic characteristics of cellulose particles, i.e. crystallinity, thermal stability, morphology, surface free energy and water vapor sorption were investigated respectively by X-ray diffraction, thermogravimetric analysis, SEM observations coupled with image analysis, contact angle measurements and dynamic vapor sorption system (DVS). It was shown that a DS as low as 0.01 was enough to drastically increase the hydrophobicity of cellulose particles without affecting the inner properties of cellulose.

1. Introduction

The research on composite materials filled with vegetal particles has sharply increased to meet the society demand for more sustainable materials. Nowadays, biocomposites combining polymers and fibers that are both bio-sourced and biodegradable are becoming serious candidates to replace conventional plastics [1]. In addition to being largely available and renewable, cellulose resources provide many benefits due to their inherent characteristics such as low density, non-abrasivity and high availability at low cost [2]. The incorporation of cellulose-based fillers in polymer matrices has one major technical bottleneck, namely the hydrophilic nature of fillers that contrasts with the more hydrophobic nature of most polymer matrices. This strong hydrophilic character leads to two main limitations: a high moisture sensitivity and a poor compatibility between the filler and the matrix. This latter results in a weak interfacial adhesion and in a low wettability of the fillers by the matrix, making difficult the dispersion of fillers in the polymer matrices due to agglomeration into knotty masses [3–5]. Therefore, the achievement of a good filler/matrix interfacial adhesion is essential to get materials with enhanced properties, especially mechanical properties and life span [6].

To address this problem, many strategies aiming at increasing the similarity of the surface properties of the composite components have been already largely investigated. They include physical and chemical modifications of either the filler surface or the polymer matrix, or the introduction of coupling agents such as maleic anhydride [7]. The modification of the filler surface is very easy due to the presence of surface hydroxyl groups and well-known grafting reactions. Possible chemical treatments of cellulose are numerous, including esterification with carboxylic acids, anhydrides, alkyl ketene dimers, acid chlorides, transesterification with triglycerides of fatty acids, etherification with epoxides, silanization with trialkoxysilane, and carbamylation with isocyanates [2,8–11]. Modifications with covalent linkages are favored to get significant and long-lasting changes of hydrophobicity. Esterification is the most common reaction used for grafting carbon chains on hydroxyl groups and the resulting cellulose is among the most

* Corresponding author at: UMR 1208 IATE - 2 place Viala - bât. 31, F-34060 Montpellier Cedex 01, France.
E-mail addresses: gregoire.david@supagro.fr (G. David), nathalie.gontard@inra.fr (N. Gontard), david.guerin@webctp.com (D. Guerin), heux@cermav.cnrs.fr (L. Heux), jerome.lecomte@cirad.fr (J. Lecomte), sonia.boisseau@cermav.cnrs.fr (S. Molina-Boisseau), helene.coussy@umontpellier.fr (H. Angellier-Coussy).

https://doi.org/10.1016/j.eurpolymj.2019.03.002
Received 26 September 2018; Received in revised form 1 March 2019; Accepted 4 March 2019
Available online 05 March 2019

biodegradable cellulose derivatives [12]. The reaction between the hydroxyl groups present at the surface of cellulose and long chain fatty acid chlorides has been known in chemistry for decades [13]. Reactions can be implemented either in homogeneous or heterogeneous phase. In homogeneous conditions, cellulose is dissolved in suitable solvents, which damage the supramolecular structure of the cellulose resulting in the loss of its intrinsic properties [14,15]. In heterogeneous systems, a partial modification of cellulose may occur but without significant effect on its characteristics [16–18]. However, the cost and the potential toxicity of aprotic organic solvents, the implementation of such reaction in anhydrous conditions as well as the use of HCl scavengers such as pyridine, have prevented large-scale sustainable applications.

Thus there is an increasing interest for solvent-free treatments. Esterification reactions were explored by mixing directly cellulose or sawdust with fatty acids, with a displacement of the equilibrium under vacuum [19] or nitrogen flow [20]. Vapor-phase esterification with trifluoroacetic anhydrides mixed with acetic acid was first successfully applied to filter paper and tunicate cellulose film hydrophobization, thus demonstrating its interest in the paper industry [21]. Chromatogenic chemistry, also called chromatografting, is based on the propagation of long chain fatty acid chlorides vapors within porous structures, akin to the diffusion conditions encountered in gas chromatography. The residual water molecules and the generated by-products of the reaction (HCl in the case of acid chloride) are continuously removed by the gas flow, which limits the possible degradation of the substrate and the reverse hydrolysis reaction. The reaction can thus be performed without any solvent and without the need of strict anhydrous conditions or HCl scavengers. This technique was first applied on paper surfaces [22,23] and then on cellulose-based aerogels using fatty acid chlorides such as palmitoyl chloride [24–26]. Degrees of substitution (DS) between 0.1 and 2.5 were reported, but grafting was restricted to the surface of cellulose only for DS values lower than 0.4. Fumagalli et al. also showed that different reagents could be used for this process and that bi-functional reagents, such as sebacoyl chloride, reacted exclusively on nanocellulose surface [27]. Up to now, such technology has never been applied to a hundred gram batch of micrometric size cellulose particles in the form of powder. In the overall context of developing high performance biocomposites by increasing the compatibility of cellulose particles with an apolar matrix, the potential interest of such an eco-friendly gas-phase esterification has been investigated in a recent study [28]. It has been shown that this process significantly improved the hydrophobicity of the cellulosic fillers resulting in a stronger filler/matrix interfacial adhesion in the PHBV-based composite. The negative effects resulting from the incorporation of cellulose in PHBV were limited when cellulose was modified by gas-phase esterification, making possible the use of higher filler contents [28].

The present paper aims at achieving deeper knowledge on the relationships between the gas-phase esterification conditions, the degree of substitution and the resulting intrinsic properties of cellulose. For that purpose, a well-known and largely available reagent, namely palmitoyl chloride, was used. Fumagalli et al. experimental conditions [25] were adapted so that a large amount of cellulose particles (100 g) could be treated. The efficiency of the treatment was evaluated by spectroscopy technics (^{13}C NMR, FT-IR). The impact on the hydrophobicity of cellulose particles was evaluated from the measurements of contact angle with different solvents and from dynamic water vapor absorption. Key intrinsic properties of cellulose particles were also monitored (thermal stability, crystallinity, morphology) in order to assess whether bulk properties were affected by the surface grafting.

2. Materials and methods

2.1. Materials

Cellulose was supplied by Arbocel J. Rettenmaier & Söhne (France) under the reference Arbocel® (grade BE 600-10 TG) in the form of a fine powder obtained after milling and sorting from pine cellulose. Particles were characterized by a cellulose content of 99.5%, a bulk density of 0.23–0.30 $g.cm^{-3}$ (in accordance with DIN EN ISO 60), a skeletal density of 1.56 $g.cm^{-3}$, an average thickness of 15 µm and an average length of 18 µm (data given by the supplier). The specific surface, measured by the BET method, was 1.33 ± 0.02 $m^2.g^{-1}$.

Palmitoyl chloride (92% of purity) was purchased from Sigma-Aldrich. Absolute ethanol (99.9% of purity) was supplied by Meridis, and acetone (99.8% of purity) was obtained from Biosolve Chimie. All chemicals were used without any further purification.

2.2. Methods

2.2.1. Gas-phase esterification of cellulose

Before treatment, cellulose was previously dried at 60 °C overnight. Cellulose (around 100 g) was placed in nylon mesh bags that were sealed and put on a grid above the reagent in a heated vacuum reactor. The reagent, palmitoyl chloride, was introduced at 0.2 eq compared to anhydroglucose units (AGU) and so in excess compared to surface hydroxyl groups. The 2 L reactor was connected to a vacuum pump through a cold trap to reach a pressure of 2 mbar. A constant nitrogen flow was introduced in order to evacuate the by-products of the reaction, mainly gaseous hydrochloric acid. The temperature varied between 100 °C and 120 °C, and the reaction time between 3 h and 15 h. After the grafting step (Fig. 1), a Soxhlet extraction with acetone was undertaken in order to remove palmitic acid and unreacted palmitoyl chloride, and to get clean grafted cellulose samples. Resulting grafted cellulose (called C-G1, C-G2, C-G3 or C-G4 depending on the grafting conditions) was finally dried overnight at 60 °C to remove residual acetone. A control sample (called C-control) was prepared without palmitoyl chloride following the same procedure including the washing step.

2.2.2. Characterization of cellulose particles

Degree of substitution. The degree of substitution (DS) represents the number of palmitoyl moieties grafted per anhydroglucose unit (AGU). As each AGU unit has 3 hydroxyl groups, the DS can thus theoretically range between 0 and 3. Here, the DS of the grafted cellulose was determined by ^{13}C NMR and confirmed by FT-IR analysis. **Solid-state ^{13}C NMR** analyses were performed using a Bruker Avance DSX 400 MHz spectrometer operating at 100.6 MHz for ^{13}C. The

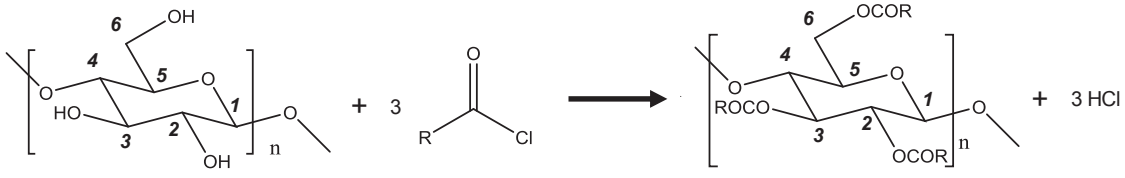

Fig. 1. Esterification of cellulose with an acyl chloride.

combination of cross-polarization, high-power proton decoupling and magic angle spinning (CP/MAS) method was used. Standard conditions were 2000 scans with 2 ms of contact and 2 s of recycle delay. The acquisition time was 35 ms and the sweep width was 29400 Hz. For DS determination, integrals were normalized with respect to area of cellulose C1 resonance peak. The infrared spectrum from **attenuated total reflectance-Fourier transform infrared analysis (ATR-FTIR)** of cellulose was recorded using a Nexus 6700 spectrophometer (ThermoElectron Corp.) equipped with a laser source HeNe and a nitrogen-cooled MCT detector. The spectra were obtained by accumulation of 32 scans with a resolution of 2 cm^{-1} in the 500–4000 cm^{-1} range. The data processing was performed using the Omnic v7.3 software. The spectra were normalized with respect to the cellulose backbone peak height, which was invariant from one sample to another. Samples were analyzed in triplicate.

2.2.2.1. X-ray diffraction analysis. Wide angle X-ray diffraction analysis was applied to assess the impact of the treatment on the crystallinity of cellulose, using an in-house setup of the laboratory Charles Coulomb, University Montpellier 2, France. An ultralow divergent beam (0.5 mrad; flux: 20 MPhotons/s; size at sample: 0.36 mm^2) was delivered by a high brightness low power X-ray tube coupled with aspheric multilayer optic (Genix^{3D} from Xenocs). The samples were in glass capillaries. In transmission configuration, scattered intensity was measured by a 2D pixel "Pilatus" detector. The signals were then analyzed with the software Fit2D. The measurements were carried out in 2θ ranges between 5° and 25° with a step size of 0.047°. The crystallinity index (CrI) of the cellulose was calculated (Eq. (1)) according to the Segal method [29]:

$$CrI\,(\%) = (I_{002} - I_{am})/I_{002} \times 100 \quad (1)$$

where I_{002} is the maximum intensity of the 002 lattice reflection of the cellulose crystallographic form at 2θ = 22° and I_{am} the diffraction intensity of the amorphous material at 2θ = 18°.

2.2.2.2. Thermogravimetric analysis. Thermogravimetric analysis (TGA) was carried out with a Mettler TGA2 apparatus equipped with a XP5U balance with a 0.1 µg resolution. Experiments were performed in triplicate. Samples (40 mg) were heated from 25 °C up to 800 °C at a rate of 10 °C.min^{-1} under a nitrogen flow (50 mL.min^{-1}). The temperature of thermal decomposition (T_{deg}) corresponded to the temperature at which the degradation rate was maximum. The temperature corresponding to the beginning of the main thermal degradation (T_{onset}) was measured when the first derivative of the weight loss became higher than 0.1%.°C^{-1}. Likewise, the offset temperature (T_{offset}) was taken at the end of derivative weight loss degradation peak when the first derivative of the weight loss became lower than 0.1% °C^{-1}.

2.2.2.3. Scanning electron microscopy (SEM). SEM was performed with a high-resolution field emission gun (SEM S-4800, Hitachi, Japan) with an acceleration voltage of 2 kV. The samples were coated with Pt by cathode pulverization.

2.2.2.4. Cellulose particle morphology. Cellulose particles were dispersed in ethanol (0.35 g.L^{-1}) and dropped on glass slides. Observations were done with an AZ100 macroscope (Nikon, JP) operating in the light transmission mode. Mosaic images were assembled with 5 × 5 images using NIS-Elements software (Nikon, JP). Images were treated using the Image J software to evaluate the polydispersity of the particles size. The software viewed each particle as an ellipse and measured major and minor axes from which d_{10}, d_{50}, d_{90} and span values were calculated. Circularity was calculated as square of the ratio between the perimeter of the particle and the circumference of a circle with the same area. A circularity value of 1.0 indicates a perfect circle.

2.2.2.5. Contact angle measurements and surface free energy. A hydraulic press (Perkin-Elmer) was used to form 13 mm diameter compact disc tablets of 0.1 g of cellulose and about 700 µm thickness, with a disc mold under pressure. Cellulose tablets were dried over P_2O_5 under vacuum for 1 h before analysis. Contact angle measurements were carried out at 23 °C using a goniometer instrument (Digidrop, GBX, France) coupled to the Windrop software (GBX, France). Five reference liquids (distilled water, ethylene glycol, diiodomethane, formamide and glycerol) were used. A drop of 3 µL was deposited on the surface of tablets and contact angles were measured as soon as the drop spreading was stabilized. Five measurements were done for each sample and each liquid. Surface free energy values were calculated using the Owens-Wendt model [30].

2.2.2.6. Dynamic vapor sorption. Water vapor sorption kinetics were performed at 20 °C using a controlled atmosphere micro-balance (DVS, Surface Measurement System Ltd., London, UK), which enables recording the water vapor uptake of the materials as a function of time for successive relative humidity (RH) steps (0, 10, 20, 30, 40, 50, 60, 70, 80, 90 and 95%). The sample was first dried at 60 °C in an oven and then dried over P_2O_5 in a desiccator and finally placed in the DVS apparatus at 0% RH for 5 h at 20 °C. Around 1 mg of cellulose particles were deposited in the form of a monolayer powder bed. Water vapor sorption isotherms were established from the equilibrium moisture contents at each RH step. Tests were performed in duplicate.

3. Results and discussion

3.1. Quantification of the gas-phase esterification efficiency

On the basis of what was already done on aerogels using this esterification method [24,25], different conditions of temperature and reaction time were tested (Table 1). The aim was not to optimize this reaction, but to understand its effect on micro-sized cellulosic particles. The occurrence of the grafting was quantified by the calculation of the degree of substitution (DS) from solid-state ^{13}C NMR results and it was further confirmed by FT-IR analysis. Results are gathered in Table 1.

DS values were calculated by solid-state ^{13}C NMR spectroscopy (Fig. 2) from peaks assigned according to the literature data [31]. The occurrence of the grafting was evidenced by the appearance of new peaks in the spectra of the modified cellulose, i.e. carboxylic carbons at 172 ppm and aliphatic carbons between 10 and 40 ppm. The degree of substitution was calculated from Eq. (2) and Eq. (3) using these two features and the integral of carbon C1 as cellulose reference:

Table 1
Degree of substitution calculated from ^{13}C NMR and FT-IR experiments for different experimental conditions (duration and temperature).

Codification	Experimental conditions (duration, temperature)	$DS_{C=O}$ (^{13}C NMR)	DS_{C-H} (^{13}C NMR)	$DS_{estimated}$ (FT-IR)
C-virgin	No grafting	–	–	–
C-control	3 h − 100 °C without reagent	–	–	–
C-G1	3 h − 100 °C	0.01	0.01	0.01 ± 0.00
C-G2	15 h − 100 °C	0.02	0.02	0.04 ± 0.00
C-G3	7 h − 120 °C	0.07	0.09	0.13 ± 0.01
C-G4	15 h − 120 °C	0.13	0.14	0.23 ± 0.01

$$DS_{C-H} = I_{C-H}/(15 \times I_{C1}) \quad (2)$$

$$DS_{C=O} = I_{C=O}/(1 \times I_{C1}) \quad (3)$$

There were only slight differences between $DS_{C\text{-}H}$ and $DS_{C=O}$. For low DS, $DS_{C\text{-}H}$ was likely more suitable since integral of carboxylic resonance signal was very low and might lead to approximations. Results from Table 1 showed that DS displayed some proportionality to reaction time and temperature, as already described in such reactions [24,25]. Grafted celluloses were obtained with DS varying from 0.01 to 0.14. These DS were lower than the ones reported by previous works: 0.15–2.7 [24] and 0.04–2.36 [25] using a similar vapor treatment. This was explained by the fact that the specific surface area of cellulose particles considered in the present study (1.33 $m^2.g^{-1}$) was much lower than that of aerogel (100 $m^2.g^{-1}$), resulting in a lower availability of surface hydroxyl groups. The comparison with DS values obtained from other treatments was delicate because of the absence of specific surface data of the substrate.

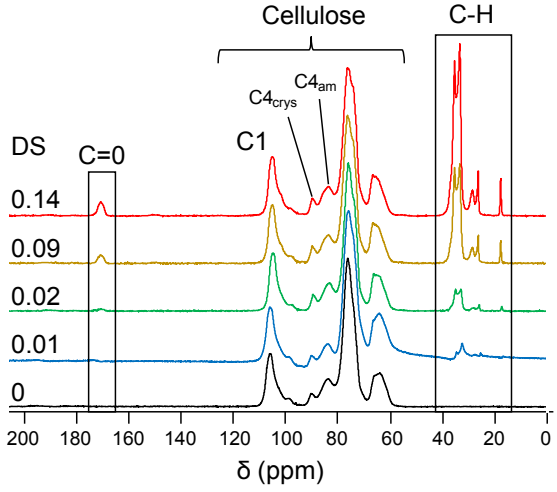

Fig. 2. Solid ^{13}C NMR spectra of virgin cellulose (DS = 0) and modified cellulose (DS = 0.01–0.14).

DS values were corroborated by FT-IR analysis. Virgin cellulose displayed a typical IR spectrum, which was mainly characterized by a broad band between 3000 and 3600 cm^{-1} corresponding to O—H groups, a peak around 2900 cm^{-1} corresponding to C—H bonds and a series of peaks between 950 and 1200 cm^{-1} corresponding to C—O bonds of the cellulose skeleton [32] (Fig. 3). The grafting of cellulose by esterification was clearly visible with the appearance of the ester carboxyl signal at 1745 cm^{-1} together with the intensity decrease of the hydroxyl parts (3000–3600 cm^{-1}). This highlighted that hydroxyl groups of cellulose reacted with palmitoyl chloride to form covalent ester bonds [25,27]. Palmitoyl chloride being a sixteen carbons compound, its grafting on cellulose also resulted in an increase of the intensity of the peaks around 2900 cm^{-1} and in the appearance of a new band around 710 cm^{-1} ascribed to CH_2 vibrations of aliphatic chains. An estimation of the degree of substitution was calculated from the intensity of the C═O stretching band (I_{1745}) and the intensity of the C—O stretching of cellulose backbone (I_{1030}) measured at 1745 cm^{-1} and 1030 cm^{-1}, respectively (Eq. (4)).

$$DS_{estimated} = I_{1475}/I_{1030} \quad (4)$$

As expected, DS from FT-IR analysis were higher than those from ^{13}C NMR, especially for the highest DS because ATR technique allows the analysis of the sample surface and does not take into account the ungrafted cellulose bulk. That is the reason why FT-IR is more used as a qualitative rather than a quantitative method.

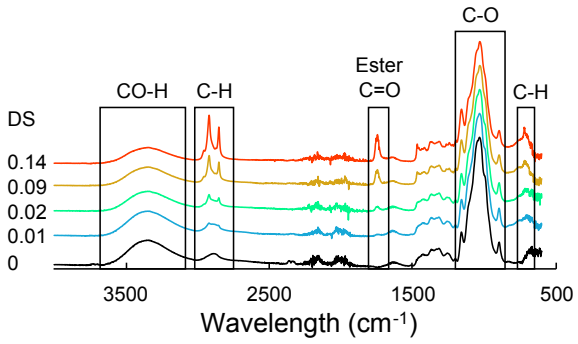

Fig. 3. FT-IR spectra of the modified celluloses with different DS.

Knowing native cellulose dimensions, it can be assumed that there is one hydroxyl group every 0.5 × 0.5 nm at the surface [33]. So, 4.10^{18} m^{-2} is the density of hydroxyl groups (d_{OH}), namely the number of OH groups per unit of surface. Knowing the specific surface area of cellulose particles (SSA), the molecular mass of anhydroglucose unit (M_{AGU}) and the Avogadro number (N_A), a theoretical DS can be calculated as follows (Eq. (5)):

$$DS_{Surface} = SSA \times d_{OH} \times M_{AGU}/N_A \quad (5)$$

Using values of respectively 1.33 $m^2.g^{-1}$, 162 $g.mol^{-1}$ and 6.022×10^{23} mol^{-1}, a $DS_{Surface}$ value of 0.0014 was obtained. Acylation of cellulose occurring from the surface to the core [34] and all the DS obtained (Table 1) being higher than $DS_{Surface}$, it was deduced that all the OH groups available at the surface of cellulose particles were grafted even under the mildest conditions tested (C-G1). As $DS_{Surface}$ strongly depends on SSA, the obtained value was obviously lower than the one from cellulose aerogels [25].

3.2. Impact of gas-phase esterification on cellulose particles intrinsic characteristics

3.2.1. Crystallinity

The crystallinity is a key intrinsic characteristic influencing the cellulose properties. XRD (Fig. 4), as well as solid-state ^{13}C NMR

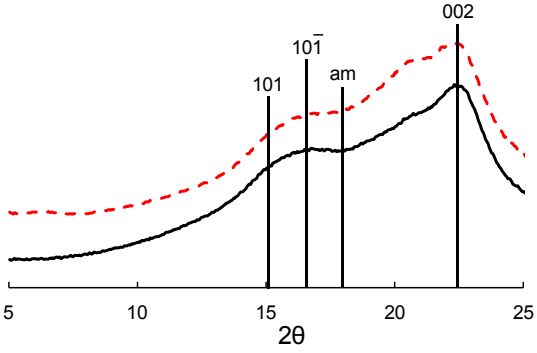

Fig. 4. X-ray diffractograms of C-virgin (–) and C-G4 (– –).

analyses were used to study the treatment effect on the cellulose crystalline structure. The Segal method is useful for quickly comparing differences between cellulose samples [29]. It is also the most usual method to determine the crystallinity index of cellulose [35]. For virgin cellulose, the typical pattern of cellulose I was displayed with 2θ peaks at 14.9, 16.3 and 22.3° that correspond to the diffraction planes 101, 10$\bar{1}$, and 002, respectively [16,36]. The cellulose considered in the present study showed a low crystallinity index, of 35 ± 3%, as compared to common cellulose fibers which usually display a crystallinity index higher than 50%. This was ascribed to the fact that the cellulose sample was obtained after successive dry grinding steps, which are well known to induce amorphization [37]. Results showed that gas-phase esterification conducted under the most drastic conditions of the present study (C-G4) did not alter significantly the crystallinity. In general, esterified cellulose with higher DS showed a progressive decrease of crystallinity [16,31]. This suggested that most of the substitutions occurred at the surface of the amorphous regions without modifying the inner structure of cellulose. This was in accordance with what was observed on ^{13}C NMR spectra (Fig. 2): the crystalline core signal ($C4_{am}$, 80–87 ppm) and amorphous chains signal ($C4_{crys}$, 87–90 ppm) did not vary within the present range of DS. The ratio of the two integrals also confirmed that the used cellulose was semi-crystalline with an important amorphous phase. The $C4_{am}$ peak gave a broader resonance due to the higher disorder and molecular mobility in the non-crystalline regions [38]. On the X-ray diffractogram of C-G4, the very slight shoulder observed at around 21° was attributed to the presence of grafted fatty chains [39].

3.2.2. Thermal stability

The thermal degradation behavior of virgin, control and grafted celluloses was investigated by thermogravimetric analysis (TGA) under nitrogen flow (Fig. 5 and Table 2). All the samples displayed a main thermal degradation step with a maximum decomposition temperature around 346 ± 1 °C for virgin and control celluloses, and 341 ± 1 °C for grafted samples. Virgin cellulose started to decompose at 260.4 ± 0.1 °C and control cellulose at 258.0 ± 0.1 °C showing a very low degradation due to the experimental conditions. Except for C-G4, which started to decompose at 251.3 ± 0.8 °C, the T_{onset} values of all grafted celluloses were around 246.5 ± 0.5 °C. Thus, there was a slight reduction of the thermal stability induced by esterification with a decrease of T_{onset} and T_{deg} for grafted celluloses compared to ungrafted celluloses (C-virgin and C-control). Normally, a small decrease of crystallinity after treatment could explain this behavior [17], which was not evidenced in section 3.2.1. The earlier thermal degradation of grafted cellulose could be thus attributed to the high lability of ester bonds [40]. However, the onset of thermal degradation temperature remained high enough, so that cellulose will not be thermally degraded during a possible future melt extrusion. It is worth noting that the thermal degradation of grafted celluloses occurred on a larger range of temperature, with T_{offset} values up to 405 °C instead of 337 °C for virgin cellulose. The degree of substitution had only a minor influence on the thermal stability.

In the case of grafted cellulose, DTG curves showed a second degradation peak at around 380 °C, the integral of which was proportional to the DS of the sample. This second degradation peak was therefore related to esterified aliphatic chains, as previously observed by Uschanov et al. [18].

Additionally, the enhancement of the hydrophobicity of grafted celluloses was confirmed by the decrease of the weight loss around 70 °C corresponding to the evaporation of absorbed water [41]. Thermogravimetric analysis showed that the differences between samples did not raise any concern about thermal stability, this validated the gas-phase esterification as a potential pre-treatment of cellulose for fillers in composite materials.

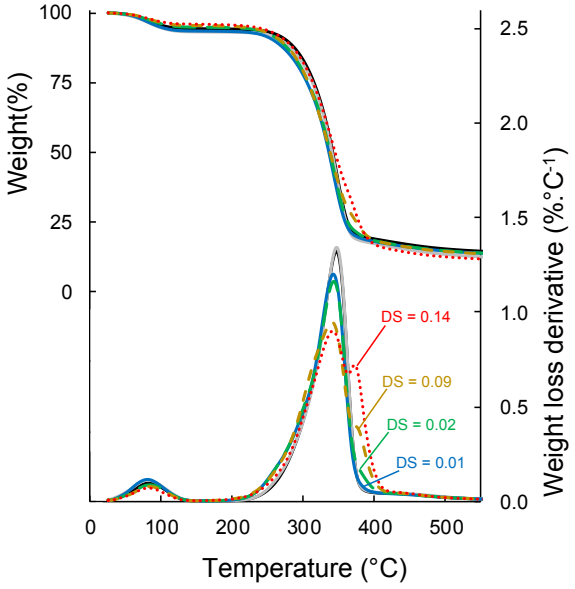

Fig. 5. TG and DTG curves of C-virgin (—), C-control (—) and grafted celluloses: C-G1, DS = 0.01 (—); C-G2, DS = 0.02 (– –); C-G3, DS = 0.09 (– –); and C-G4, DS = 0.14 (····) under N_2.

Table 2
Results of the thermogravimetric analysis.

	Tdeg (°C)	Tonset (0.1%/°C)	Toffset (0.1%/°C)
C-virgin	345.9 ± 0.3	260.4 ± 0.1	377.3 ± 0.1
C-control	346.5 ± 0.1	258.0 ± 0.1	377.0 ± 0.6
C-G1	341.1 ± 0.8	246.0 ± 0.3	378.3 ± 0.1
C-G2	342.4 ± 0.1	246.8 ± 0.4	390.3 ± 0.1
C-G3	340.5 ± 1.0	246.8 ± 0.2	400.7 ± 0.1
C-G4	341.0 ± 0.1	251.3 ± 0.8	405.6 ± 0.3

3.2.3. Cellulose particle morphology

The appearance of modified particles was observed by SEM and compared to virgin cellulose (Fig. 6). No clear difference between grafted and virgin celluloses was visible on SEM images, suggesting that no significant degradation of the macroscopic structure occurred during the treatment. This was in agreement with TGA results. At high resolution, a surface smoothness could be observed on C-G4 particles (C3) as compared to virgin cellulose (A3) or C-G1 cellulose (B3). This looked like depositions on particles; the particles seemed to be embedded in a kind of snow layer. Similar phenomenon was observed on bacterial cellulose microfibrils by Berlioz et al. [24]. It was confirmed by 2D image analysis (Table 3) that the dimensions of the particles were not significantly affected.

3.2.4. Wettability of grafted cellulose

The effect of gas-phase esterification on the cellulose surface hydrophobicity was clearly and visually evidenced by the observation of a drop of water on either the virgin or grafted cellulose (Fig. 7) and quantified by contact angle measurements (Table 4). Whatever experimental conditions used, gas-phase esterification resulted in a drastic increase of the water contact angle value, highlighting the expected targeted increase of hydrophobicity induced by the grafting. Water contact angle values increased from 44° for the virgin cellulose up to 97°–109° for grafted cellulose. Obtaining water contact angle values higher than 90°, which corroborated the hydrophobic character of grafted cellulose [42]. This was confirmed with other polar liquids. Grafted cellulose displayed a hydrophobic surface even with modest DS of 0.01. The increasing values of the contact angle with non-polar solvents such as diiodomethane indicated that the particles became

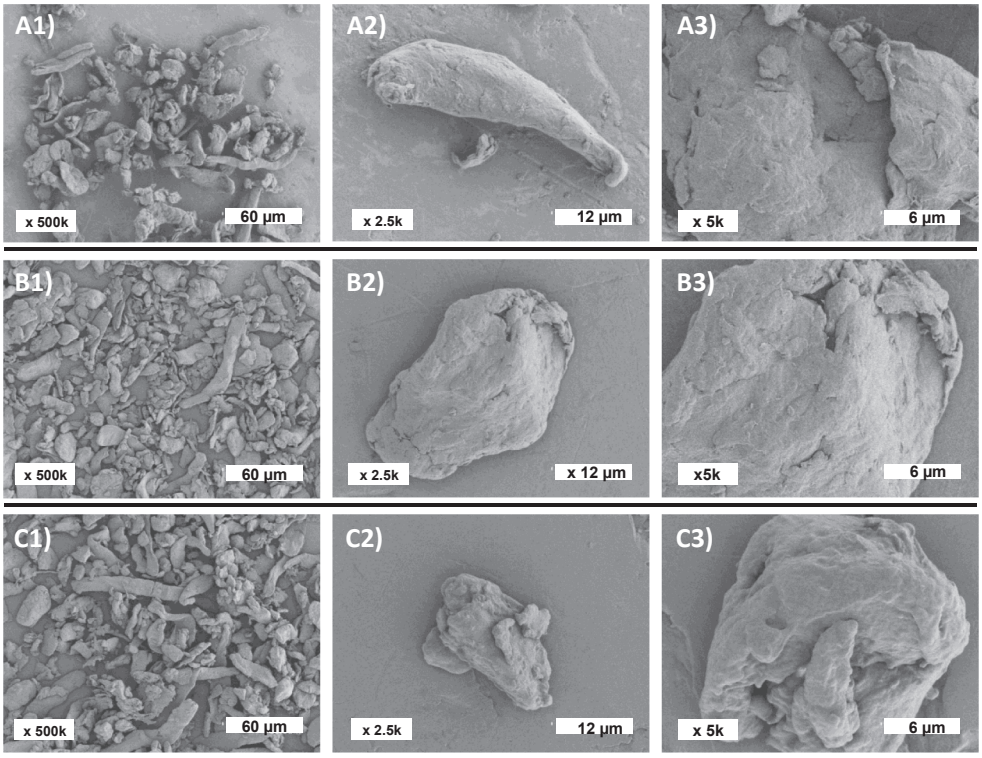

Fig. 6. SEM pictures of (A1-3) virgin cellulose C-virgin and grafted cellulose (B1-3) C-G1 and (C1-3) C-G4 particles at different magnifications.

slightly lipophobic. This double phobic character is generally found with perfluorinated materials [43]. The macroscopic behavior of the water drop on cellulose tablets depended on the nature of the cellulose surface. Grafted cellulose tablets exhibited a water repellence, with a water contact angle very stable over time, whereas the drop of water was rapidly absorbed by virgin cellulose tablets due to capillarity effects. However, no correlation between the degree of substitution and water contact angle values could be established, as already reported for long chain cellulose esters [44].

Contact angle measurements with solvents of different polarities allowed the estimation of the polar (γ^P) and dispersive (γ^d) components of the solid surface free energy (γ) of virgin and grafted celluloses using the Owens-Wendt's approach (Table 4). In all cases, the substitution of the surface hydroxyl groups by long-chain aliphatic esters after gas-phase esterification resulted in a drastic decrease of the polar component from 17.7 $mJ.m^{-2}$ down to nearly zero. This decrease might be too sharp since the objective was to reduce the polar component of cellulose to be the closest to the polymer one and not necessary to reach zero. The dispersive components of grafted celluloses exhibited a lower γ^d value (around 22 $mJ.m^{-2}$) than the virgin cellulose (32 $mJ.m^{-2}$). Such phenomenon was observed with octadecyl-silanated cellulose

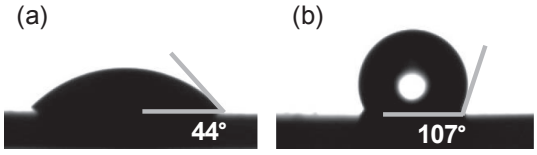

Fig. 7. Pictures of a drop of water deposited on compressed tablets constituted of (a) virgin cellulose and (b) grafted cellulose.

[45]. This is rather unexpected compared with the literature data [16,46,47] but could be explained by the low surface energy of grafted alkyl chain. The extent of grafting, reflected by the DS value, did not have a significant impact on surface free energy values, suggesting that the mildest experimental conditions used were sufficient to reach a complete hydrophobization of the cellulose surface. Since the hydrophobic character was the main target, low DS values were enough to achieve our primary goal. The DS threshold was 3×10^{-4} for acetic-oleic cellulose esters [48]. This value may change with the length of the grafted fatty chain.

Table 3
Morphological parameters in volume of C-virgin and C-G4 cellulose particles.

		d10 (µm)	d50 (µm)	d90 (µm)	Span	Circularity
C-virgin	**Major axis**	17 ± 3	40 ± 4	71 ± 5	1.4 ± 0.3	0.71 ± 0.02
	Minor axis	11 ± 2	23 ± 2	34 ± 3	1.0 ± 0.1	
C-G4	**Major axis**	19 ± 4	43 ± 2	65 ± 4	1.0 ± 0.1	0.71 ± 0.02
	Minor axis	12 ± 2	24 ± 2	36 ± 1	1.0 ± 0.2	

Table 4
Contact angle values (°), polar (γ^p) and dispersive (γ^d) components of the surface free energy (γ) of virgin cellulose (C-virgin) and grafted cellulose (C-GX) with different reference liquids.

	Contact angle (°)					Surface free energy (mJ.m^{-2})		
	Water	Ethylene glycol	Diiodomethane	Formamide	Glycerol	γ^p	γ^d	γ
C-virgin	44 ± 2	35 ± 2	33 ± 3	28 ± 3	59 ± 5	17.7	32.1	49.8
C-G1	98 ± 1	51 ± 1	36 ± 2	52 ± 0	91 ± 7	0.2	22.2	22.4
C-G2	107 ± 2	87 ± 3	64 ± 5	94 ± 2	103 ± 2	0.2	23.5	23.7
C-G3	109 ± 3	87 ± 1	57 ± 4	99 ± 2	105 ± 2	0.1	21.5	21.6
C-G4	103 ± 4	95 ± 4	57 ± 4	103 ± 4	100 ± 3	0.1	20.1	20.2

3.2.5. Water vapor sorption of grafted cellulose

The impact of chemical grafting on water vapor sorption in cellulose particles was investigated by dynamic vapor sorption (DVS) measurements (Fig. 8). Similar water sorption patterns were observed for all samples, esterified or not. Water vapor isotherms displayed a sigmoidal curve typical of cellulose-based materials [49]. The water vapor uptake gradually increased with the relative humidity, reaching at 95% RH a water vapor uptake of 0.227 ± 0.004 g.g^{-1} dry basis (d.b.) for virgin cellulose and 0.162 ± 0.005 g.g^{-1} d.b. for C-G4. The virgin cellulose values were in accordance with water vapor sorption uptake measured using a QCM device [50]. From the Park's model that usually well describes such experimental results, the isotherm curves can be divided in three parts: at RH < 10% water is sorbed by hydrogen bonding onto specific sites at the surface (part I), then at 10% < RH < 60% the water concentration increases linearly with water activity by capillarity due to the porous structure of cellulose. Finally, at RH > 60%, the water sorption increases more dramatically as a power function likely due to the capillary condensation in cellulose and to water vapor clustering effect [51,52].

Globally, except for a RH of 10%, lower equilibrium moisture uptakes were recorded for grafted samples as compared to virgin cellulose. This means that the hydrophobic carbon moieties on grafted celluloses prevented the adsorption of water vapor. It is worth noting that esterification mainly affected water vapor sorption behavior on zone II. In fact, at the beginning of this zone (RH = 10%), water uptake was the same for all cellulose samples whereas toward at the end of this zone (RH = 60%), water vapor uptake was 0.102 g.g^{-1} d.b. and 0.055 g.g^{-1} d.b. for C-virgin and for C-G4 respectively. Moisture sorption was significantly affected by the degree of substitution, with decreasing water sorption values at each RH step for increasing DS values. The difference of water sorption could not be explained by the crystallinity that remained the same, as shown previously. This result could rather be explained by the pore volume modification of the cellulose particles due to the esterification step. Similar results were previously observed on cellulose nanofibrils [53] and agave fibers [54]. This effect was more pronounced than the one already observed by Peydecastaing et al. for acetic-fatty cellulose esters [48]. In the present case, this could be explained by a longer alkyl chain grafted to the cellulose as suggested by the study of Sehaqui et al. which showed a relation between the moisture absorption and the alkyl chain length grafted. The effect of grafting was more DS dependent in the case of vapor water than with liquid water (water contact angle), because of their physical state. As explained in the study by Peydecastaing et al. [48], individual vapor water molecules could more easily reach free remaining hydroxyl groups of the cellulose than a drop of water which is a cluster of hydrogen bonded molecules.

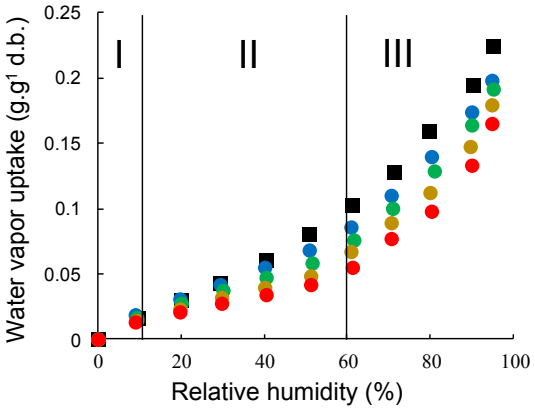

Fig. 8. Water vapor sorption isotherm of virgin cellulose: C-virgin (■) and grafted cellulose: C-G1 (●), C-G2 (●), C-G3 (●), C-G4 (●).

4. Conclusion

Gas-phase esterification of cellulose particles by fatty acid chlorides seems to be a promising approach to produce bio-based fillers tailored for the biocomposite market. The gas-phase esterification was first used on micron-size cellulose particles. This treatment was carried out to make them more hydrophobic and to avoid the main drawbacks of cellulose as fillers namely, poor compatibility with non-polar matrix and moisture absorption. The reagent was palmitoyl chloride, a well-known bio-based long-chain aliphatic acid chloride. The chosen conditions enabled the grafting of palmitoyl moieties onto the surface without degrading the intrinsic structure of cellulose. Surface free energy of grafted celluloses calculated from contact angles showed a fall of the polar component even for the lowest DS, whereas moisture sorption was significantly decreased by the cellulose DS. Cellulose integrity was checked through macroscopic observations, thermogravimetric analyses, SEM, XRD and spectrometric methods. The backbone of cellulose was not altered. Next steps would be to apply this treatment to lignocellulosic fillers. Overall, it can be concluded that gas-phase esterification is an adequate reaction to tailor the interfacial adhesion of micrometric size cellulose particles with an apolar matrix, therefore offering new perspectives in the development of novel biocomposite materials.

Acknowledgments

This work was carried out in the framework of the NoAW project, which is supported by the European Commission through the Horizon

2020 research and innovation program under the Grant Agreement No 688338. The authors would like to acknowledge Emilie Ressouche for her help and advices on the use of the reactor for gas-phase esterification.

Data availability

The data that support the findings of this study are openly available in “Exploring the potential of gas-phase esterification to hydrophobize the surface of micrometric cellulose particles _ Raw data”. at https://doi.org/10.15454/6VQ9JA.

References

[1] A.K. Mohanty, M. Misra, L.T. Drzal, Natural fibers, biopolymers, and biocomposites, Taylor Francis (2005), https://doi.org/10.1201/9780203508206.

[2] M.J. John, S. Thomas, Biofibres and biocomposites, Carbohydr. Polym. 71 (2008) 343–364, https://doi.org/10.1016/j.carbpol.2007.05.040.

[3] R.G. Raj, B.V. Kokta, F. Dembele, B. Sanschagrain, Compounding of cellulose fibers with polypropylene: Effect of fiber treatment on dispersion in the polymer matrix, J. Appl. Polym. Sci. 38 (1989) 1987–1996, https://doi.org/10.1002/app.1989.070381103.

[4] K.L. Pickering, M.G.A. Efendy, T.M. Le, A review of recent developments in natural fibre composites and their mechanical performance, Compos. Part A Appl. Sci. Manuf. 83 (2016) 98–112, https://doi.org/10.1016/j.compositesa.2015.08.038.

[5] O. Faruk, M. Sain, Biofiber reinforcement in composite materials, Woodhead Publishing, Cambridge, 2015.

[6] C. Fonseca-Valero, A. Ochoa-Mendoza, J. Arranz-Andrés, C. González-Sánchez, Mechanical recycling and composition effects on the properties and structure of hardwood cellulose-reinforced high density polyethylene eco-composites, Compos. Part A Appl. Sci. Manuf. 69 (2015) 94–104, https://doi.org/10.1016/j.compositesa.2014.11.009.

[7] J. George, M.S. Sreekala, S. Thomas, A review on interface modification and characterization of natural fiber reinforced plastic composites, Polym. Eng. Sci. 41 (2001) 1471–1485, https://doi.org/10.1002/pen.10846.

[8] O. Faruk, A.K. Bledzki, H.P. Fink, M. Sain, Biocomposites reinforced with natural fibers: 2000–2010, Prog. Polym. Sci. 37 (2012) 1552–1596, https://doi.org/10.1016/j.progpolymsci.2012.04.003.

[9] M.A. Hubbe, O.J. Rojas, L.A. Lucia, Green modification of surface characteristics of cellulosic materials at the molecular or nano scale : a review, BioResources. 10 (2015) 6095–6206.

[10] A.K. Bledzki, J. Gassan, Composites reinforced with cellulose based fibers, Prog. Polym. Sci. 24 (1999) 221–274, https://doi.org/10.1016/S0079-6700(98)00018-5.

[11] Ana Gisela Cunha, Alessandro Gandini, Turning polysaccharides into hydrophobic materials: a critical review. Part 1. cellulose, Cellulose 17 (5) (2010) 875–889, https://doi.org/10.1007/s10570-010-9434-6.

[12] O.A. El Seoud, T. Heinze, Organic esters of cellulose: New perspectives for old polymers, Adv. Polym. Sci. 186 (2005) 103–149, https://doi.org/10.1007/b136818.

[13] G.D. Hiatt, C.L. Crane, Method of preparing higher fatty acid esters of cellulose, 1941.

[14] C.L. McCormick, D.K. Lichatowich, J.A. Pelezo, K.W. Anderson, Homogeneous solution reactions of cellulose, chitin, and other polysaccharides, J. Polym. Sci. Part C Polym. Lett. 17 (1979) 479–484, https://doi.org/10.1021/bk-1980-0121.ch024.

[15] C. Vaca-Garcia, S. Thiebaud, M.E. Borredon, G. Gozzelino, Cellulose esterification with fatty acids and acetic anhydride in lithium chloride/N, N-dimethylacetamide medium, J. Am. Oil Chem. Soc. 75 (1998) 315–319, https://doi.org/10.1007/s11746-998-0047-2.

[16] C.S.R. Freire, A.J.D. Silvestre, C.P. Neto, M.N. Belgacem, A. Gandini, Controlled heterogeneous modification of cellulose fibers with fatty acids: effect of reaction conditions on the extent of esterification and fiber properties, J. Appl. Polym. Sci. 100 (2006) 1093–1102, https://doi.org/10.1002/app.23454.

[17] P. Jandura, B. Riedl, B.V. Kokta, Thermal degradation behavior of cellulose fibers partially esterified with some long chain organic acids, Polym. Degrad. Stab. 70 (2000) 387–394, https://doi.org/10.1016/S0141-3910(00)00132-4.

[18] P. Uschanov, L.-S. Johansson, S.L. Maunu, J. Laine, Heterogeneous modification of various celluloses with fatty acids, Cellulose 18 (2011) 393–404, https://doi.org/10.1007/s10570-010-9478-7.

[19] H.S. Kwatra, J.M. Caruthers, B.Y. Tao, Synthesis of long chain fatty acids esterified onto cellulose via the vacuum-acid chloride process, Ind. Eng. Chem. Res. 31 (1992) 2647–2651, https://doi.org/10.1021/ie00012a004.

[20] S. Thiebaud, M.E. Borredon, Solvent-free wood esterification with fatty acid chlorides, Bioresour. Technol. 52 (1995) 169–173, https://doi.org/10.1016/0960-8524(95)00018-A.

[21] H. Yuan, Y. Nishiyama, S. Kuga, Surface esterification of cellulose by vapor-phase treatment with trifluoroacetic anhydride, Cellulose 12 (2005) 543–549, https://doi.org/10.1007/s10570-005-7136-2.

[22] C. Stinga, D. Guerin, D. Samain, Development of biocompatible flexible films with high barriers properties against water, grease and gases using smart reacto-chromatogenic nanoparticles, Adv. Coat. Fundam. Symp. (2012).

[23] D. Samain, Procédé de traitement d’un matériau solide pour le rendre hydrophobe, matériau obtenu et applications., PCT patent 98.942743.0, 1998.

[24] S. Berlioz, S. Molina-Boisseau, Y. Nishiyama, L. Heux, Gas-phase surface esterification of cellulose microfibrils and whiskers, Biomacromolecules 10 (2009) 2144–2151, https://doi.org/10.1021/bm900319k.

[25] M. Fumagalli, D. Ouhab, S.M. Boisseau, L. Heux, Versatile gas-phase reactions for surface to bulk esterification of cellulose microfibrils aerogels, Biomacromolecules. 14 (2013) 3246–3255, https://doi.org/10.1021/bm400864z.

[26] M. Fumagalli, F. Sanchez, S.M. Boisseau, L. Heux, Gas-phase esterification of cellulose nanocrystal aerogels for colloidal dispersion in apolar solvents, Soft Matter. 9 (2013) 11309–11317, https://doi.org/10.1039/c3sm52062e.

[27] M. Fumagalli, F. Sanchez, S. Molina-Boisseau, L. Heux, Surface-restricted modification of nanocellulose aerogels in gas-phase esterification by di-functional fatty acid reagents, Cellulose 22 (2015) 1451–1457, https://doi.org/10.1007/s10570-015-0585-3.

[28] G. David, N. Gontard, H. Angellier-Coussy, Mitigating the impact of cellulose particles on the performance of biopolyester-based composites by gas-phase esterification, Polym. (Basel) 11 (2019), https://doi.org/10.3390/polym11020200.

[29] L. Segal, J.J. Creely, A.E. Martin, C.M. Conrad, Empirical method for estimating the degree of crystallinity of native cellulose using the X-ray diffractometer, Text. Res. J. 29 (1959) 786–794, https://doi.org/10.1177/004051755902901003.

[30] D. Owens, R. Wendt, Estimation of the surface free energy of polymers, J. Appl. Polym. Sci. 13 (1969) 899–928, https://doi.org/10.1002/app.1969.070130815.

[31] P. Jandura, B.V. Kokta, B. Riedl, Fibrous long-chain organic acid cellulose esters and their characterization by diffuse reflectance FTIR spectroscopy, solid-state CP/MAS 13C-NMR, and X-ray diffraction, J. Appl. Polym. Sci. 78 (2000) 1354–1365, https://doi.org/10.1002/1097-4628(20001114)78:7<1354::AID-APP60>3.0.CO;2-V.

[32] Y. Marechal, H. Chanzy, The hydrogen bond network in Iβ cellulose as observed by infrared spectrometry, J. Mol. Struct. 523 (2000) 183–196, https://doi.org/10.1016/S0022-2860(99)00389-0.

[33] M. Wada, T. Okano, J. Sugiyama, Synchrotron-radiated X-ray and neutron diffraction study of native cellulose, Cellulose. 4 (1997) 221–232, https://doi.org/10.1023/A:1018435806488.

[34] R.E. Glegg, D. Ingerick, R.R. Parmerter, J.S.T. Salzer, R.S. Warburton, Acetylation of cellulose I and II studied by limiting viscosity and X-ray diffraction, J. Polym. Sci. Part A-2 Polym. Phys. 6 (1968) 745–773, https://doi.org/10.1002/pol.1968.160060410.

[35] S. Park, J.O. Baker, M.E. Himmel, P.A. Parilla, D.K. Johnson, Cellulose crystallinity index : measurement techniques and their impact on interpreting cellulase performance, Biotechnol. Biofuels. 3 (2010) 1–10, https://doi.org/10.1186/1754-6834-3-10.

[36] Z. Hu, R.M. Berry, R. Pelton, E.D. Cranston, One-pot water-based hydrophobic surface modification of cellulose nanocrystals using plant polyphenols, ACS Sustain. Chem. Eng. 5 (2017) 5018–5026, https://doi.org/10.1021/acssuschemeng.7b00415.

[37] B.N. Stubicar, I. Smit, M. Stubicar, A. Tonejc, A. Janosi, J. Schurz, P. Zipper, An X-ray diffraction study of the crystalline to amorphous phase change in cellulose during high-energy dry ball milling, Holzforschung 52 (1998) 455–458, https://doi.org/10.1515/hfsg.1998.52.5.455.

[38] R.H. Atalla, D.L. Vanderhart, The role of solid state C-13 NMR spectroscopy in studies of the nature of native celluloses, Solid State Nucl. Magn. Reson. 15 (1999) 1–19, https://doi.org/10.1016/s0926-2040(99)00042-9.

[39] A. Junior De Menezes, G. Siqueira, A.A.S. Curvelo, A. Dufresne, Extrusion and characterization of functionalized cellulose whiskers reinforced polyethylene nanocomposites, Polym. (Guildf) 50 (2009) 4552–4563, https://doi.org/10.1016/j.polymer.2009.07.038.

[40] L.C. Tomé, M.G. Freire, L.P.N. Rebelo, A.J.D. Silvestre, C.P. Neto, I.M. Marrucho, C.S.R. Freire, Surface hydrophobization of bacterial and vegetable cellulose fibers using ionic liquids as solvent media and catalysts, Green Chem. 13 (2011) 2464, https://doi.org/10.1039/c1gc15432j.

[41] S. Soares, G. Camino, S. Levchik, Comparative study of the thermal decomposition of pure cellulose and pulp paper, Polym. Degrad. Stab. 49 (1995) 275–283, https://doi.org/10.1016/0141-3910(95)87009-1.

[42] L. Feng, S. Li, Y. Li, H. Li, L. Zhang, J. Zhai, Y. Song, B. Liu, L. Jiang, D. Zhu, Superhydrophobic surfaces: From natural to artificial, Adv. Mater. 14 (2002) 1857–1860, https://doi.org/10.1002/adma.200290020.

[43] A.G. Cunha, C.S.R. Freire, A.J.D. Silvestre, C.P. Neto, A. Gandini, Reversible hydrophobization and lipophobization of cellulose fibers via trifluoroacetylation, J. Coll. Interf. Sci. 301 (2006) 333–336, https://doi.org/10.1016/j.jcis.2006.04.078.

[44] J. Peydecastaing, S. Girardeau, C. Vaca-Garcia, M.E. Borredon, Long chain cellulose esters with very low DS obtained with non-acidic catalysts, Cellulose 13 (2005) 95–103, https://doi.org/10.1007/s10570-005-9012-5.

[45] W. Tze, M.E.P. Walinder, D.J. Gardner, Inverse gas chromatography for studying interactions of materials used for cellulose fiber/polymer composites, J. Adhes. Sci. Technol. 20 (2006) 743–759, https://doi.org/10.1163/156856106777638644.

[46] C. Gaiolas, M.N. Belgacem, L. Silva, W. Thielemans, A.P. Costa, M. Nunes, M.J. Santos Silva, Green chemicals and process to graft cellulose fibers, J. Coll. Interf. Sci. 330 (2009) 298–302, https://doi.org/10.1016/j.jcis.2008.10.059.

[47] D. Pasquini, M. Naceur, A. Gandini, Surface esterification of cellulose fibers : characterization by DRIFT and contact angle measurements, J. Coll. Interf. Sci. 295 (2006) 79–83, https://doi.org/10.1016/j.jcis.2005.07.074.

[48] J. Peydecastaing, C. Vaca-Garcia, E. Borredon, Interactions with water of mixed acetic-fatty cellulose esters, Cellulose 18 (2011) 1023–1031, https://doi.org/10.1007/s10570-011-9530-2.

[49] S. Brunauer, L.S. Deming, W.E. Deming, E. Teller, On a Theory of the van der Waals adsorption of gases, J. Am. Chem. Soc. 62 (1940) 1723–1732, https://doi.org/10.

1021/ja01864a025.
[50] V. Thoury-Monbrun, S. Gaucel, V. Rouessac, V. Guillard, H. Angellier-Coussy, Assessing the potential of quartz crystal microbalance to estimate water vapor transfer in micrometric size cellulose particles, Carbohydr. Polym. 190 (2018) 307–314, https://doi.org/10.1016/j.carbpol.2018.02.068.
[51] G. Banik, I. Brückle, Principles of water absorption and desorption in cellulosic materials, Restaur. Int. J. Preserv. Libr. Arch. Mater. 31 (2010) 164–177, https://doi.org/10.1515/rest.2010.012.
[52] A. Célino, O. Gonçalves, F. Jacquemin, S. Fréour, Qualitative and quantitative assessment of water sorption in natural fibres using ATR-FTIR spectroscopy, Carbohydr. Polym. 101 (2014) 163–170, https://doi.org/10.1016/j.carbpol.2013.09.023.
[53] H. Sehaqui, T. Zimmermann, P. Tingaut, Hydrophobic cellulose nanopaper through a mild esterification procedure, Cellulose 21 (2014) 367–382, https://doi.org/10.1007/s10570-013-0110-5.
[54] A. Bessadok, D. Langevin, F. Gouanvé, C. Chappey, S. Roudesli, S. Marais, Study of water sorption on modified Agave fibres, Carbohydr. Polym. 76 (2009) 74–85, https://doi.org/10.1016/j.carbpol.2008.09.033.